Journal of
Ceramic Science
and Technology

J. Ceram. Sci. Tech., **01** [01] 27-31 (2010)
DOI: 10.4416/JCST2010-00006
available online at: http://www.ceramic-science.com

Effect of Co Co-Doping on the Densification and Electrical Conductivity of $Ce_{0.9}Sm_{0.1}O_{2-\delta}$ Solid Electrolytes

M.J. Pawar, S.S. Chaure, S.B. Deshmukh

Laboratory of Materials Synthesis, Department of Chemistry, ACS College, Amravati, India, 444602
received March 23, 2010; received in revised form May 26, 2010; accepted May 30, 2010

Abstract

The influence of cobalt doping on the densification and activation energy of $Ce_{0.9}Sm_{0.1}O_{2-\delta}$ was studied. Solid solutions of $Ce_{0.9-x}Co_xSm_{0.1}O_{2-\delta}$ (x = 0, 0.05, 0.1 and 0.15) were prepared by means of a modified EDTA-glycol method. It was found that the degree of densification increases with an increasing concentration of cobalt. Almost full densification could be achieved at a sintering temperature of 1500 °C. The highest density (99.3 %) and minimum activation energy (0.81 eV) were observed for the composition $Ce_{0.8}Co_{0.1}Sm_{0.1}O_{2-\delta}$.

Keywords: SOFC; ceria; EDTA-glycol method; co-dopant; solid electrolytes

I. Introduction

Solid oxide fuel cells (SOFCs) have high power generating efficiency and are applicable to a wide range of power supplies, from small-scale distribution power supplies to large-scale thermal power generation. Low pollution, high power densities, flexibility in using hydrocarbon fuels are the advantages of SOFCs[1] as they are considered as the premium power sources for the future. SOFCs operating at intermediate temperature (< 800 °C) have received increasing attention as the low operating temperatures prolong the service life of SOFCs and reduce the cost of materials processing and cell fabrication[2]. Solid oxide electrolyte is a key component of SOFCs, affecting cell performance and operating temperature to a large extent. Solid oxide electrolytes based on ceria-doped materials with sufficient electrical properties are studied as promising candidate materials for use in intermediate-temperature solid oxide fuel cells (IT-SOFCs).

At present, doped ceria with a cubic structure exhibits the highest ionic conductivity in the range of 450-750 °C. The high ionic conductivity in doped ceria arises from charge-compensating oxygen vacancies related to aliovalent cation conditions[3]. Ceria-based solid electrolytes doped with various cations like La^{3+}, Gd^{3+}, Sm^{3+}, Pr^{3+} etc., at different dopant concentrations have been extensively investigated in order to obtain an electrolyte with high ionic conductivity at reduced temperature. Trivalent cation enhances the chemical stability and the ionic conductivity while suppressing the reducibility of ceria-based materials. Among the various dopants studied, gadolinia-doped ceria (GDC) and samarium-doped ceria (SDC) have been reported to exhibit the highest ionic conductivity[4]. SDC materials show high ionic conductivity[5-7], this is because, as a dopant, Sm^{3+} cations minimize the change in the ceria lattice. In addition to descriptions of singly doped ceria, many studies have reported on co-doped samples and results suggest that co-doping may enhance conductivity even at moderate or intermediate temperatures[8-11]. Oxides of transition metal (e.g. Fe_2O_3, Co_2O_3, SrO_2, etc.) are some of the co-dopants suggested for decreasing the sintering temperature as well as for enhancing the ionic conductivity of ceria-based solid electrolytes. Co has previously been suggested as a sintering aid for CeO_2[12]. M. A. Azimova et al. reported that Co doping is an effective technique for reducing the sintering temperature required to form dense ceramics[13].

In this work, cobalt co-doped $Ce_{0.9}Sm_{0.1}O_{2-\delta}$ nanopowders were synthesized. The effect of the Co_2O_3 co-doping on crystallite size, relative density and activation energy was investigated.

II. Experimental

The pure and Co-doped $Ce_{0.9}Sm_{0.1}O_{2-\delta}$ materials were prepared by means of a modified EDTA-glycol method[14]. Highly pure $Ce(NO_3)_3.6H_2O$, $Sm(NO_3)_3.6H_2O$ and $Co(NO_3)_2.6H_2O$ were used as the precursors. These salts were mixed independently in de-ionized water. Later all the solutions were mixed in the correct ratio in order to form the solid solution of $Ce_{0.9-x}Co_xSm_{0.1}O_{2-\delta}$ with x = 0, 0.05, 0.1 and 0.15 composition. The calculated quantities of ethylenediaminetetraacetic acid (EDTA), dilute ammonia and ethylene glycol (EG) were added to the nitrate solution. The solution so formed was stirred and kept on a hot plate for heat treatment at 80 °C until it formed a gel-like mass. The resulting mass was combusted at 300 °C for 2 h, and then calcined at 650 °C for 7 h. The ashes obtained from calcination were ground in an agate mortar in order to obtain homogeneous powders. The powders were uniaxially pressed at 200 MPa into pellets with a diameter of 6 mm and a thickness of 2 mm. The pellets were sintered in air for 7 h at a constant heating rate (CHR) of 2 °C/min between 1350 °C and 1550 °C.

* Corresponding author: pawarmj@hotmail.com

The phase composition was examined with X-ray diffraction (XRD). The values for the specific surface areas (S_{BET}) of the calcined powders were measured with the Brunauer-Emmett-Teller (BET) nitrogen-gas adsorption method. The densities of green and sintered pellets were calculated from the mass and dimensions of the samples, and measured with the Archimedes method in a water bath. The microstructures of the powders and sintered samples were examined with a scanning electron microscope (SEM). The average grain size was measured with the intercept method on the surface of polished and thermally etched sintered samples. The size of at least 300 grains was taken into account. The electrical conductivity of the samples was measured by applying the impedance spectroscopy method. The conductivity measurements were conducted at different temperatures in the range 300-700°C in air. Each side of the sample was coated with silver paste and the coatings were then dried to produce solid silver electrode on both sides of the pellet.

III. Results and discussion

All the $Ce_{0.9-x}Sm_{0.1}Co_xO_{2-\delta}$ powders were characterized with X-ray diffraction techniques and the XRD patterns are presented in fig. 1. All the samples exhibit a characteristic fluorite structure. A gradual enlargement of the

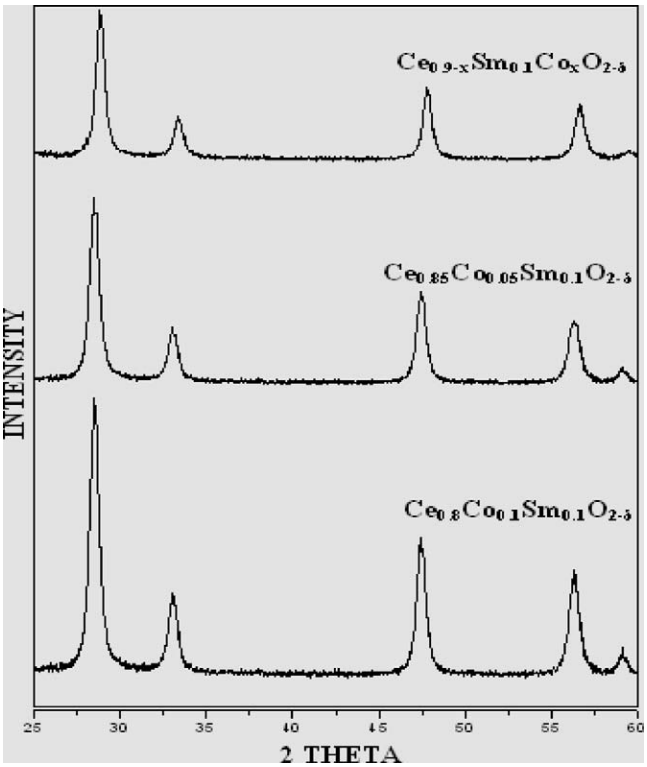

Fig. 1: XRD patterns of ceria-based powders.

XRD peaks for all the samples was observed with increasing cobalt concentration. In general, a broadening of peaks indicates a reduction in crystallite size. The diffraction pattern of all the Co co-doped powders was observed to be similar to that of $Ce_{0.9}Sm_{0.1}O_{2-\delta}$ powders. No extra peaks were observed for Sm_2O_3 or Co_2O_3. This indicates that cobalt ions had properly dissolved in the $Ce_{0.9}Sm_{0.1}O_{2-\delta}$ into the Sm site and a homogeneous solid solution had formed. It is generally accepted that synthesis of ceramics based on the wet-chemical method is preferred to those methods employing reactions in the solid state, because it gives rise to more homogeneous powders with controlled composition. The crystallite size (D) was calculated with the Scherrer equation (Eq. 1);

$$D = 0.9\lambda/\beta \cos\theta \quad (1)$$

where λ is a wavelength of the radiation, β is full width at half maxima (FWHM) and θ is the diffraction angle. Fig. 2 shows the effect of cobalt concentration on the average crystallite size of $Ce_{0.9-x}Sm_{0.1}Co_xO_{2-\delta}$ samples calcined at 650 °C. It can be seen that the crystallite size (calculated from the Scherrer equation) decreases with increasing cobalt concentration. Table 1 shows the lattice parameter (a) and the average crystallite size (D) of the samples synthesized with the EDTA-glycol method. It was found that the unit-cell lattice parameter of $Ce_{0.9-x}Co_xSm_{0.1}O_{2-\delta}$ solid electrolytes decreases steadily with increasing cobalt concentration (fig. 3). Such a decrease in the unit-cell parameter can be attributed to the replacement of bigger Ce^{4+} ions (0.96 Å) by smaller Co^{2+} ions (0.83 Å). From the experimental results, it was concluded that Co_2O_3 is soluble in a solution of Sm-doped ceria.

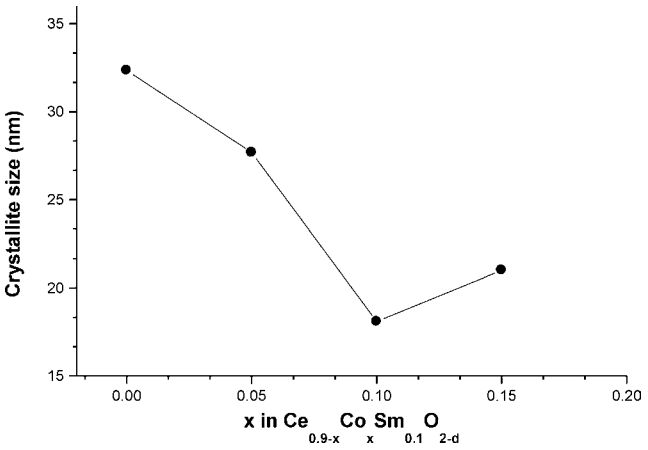

Fig. 2: Crystallite sizes of $Ce_{0.9-x}Co_xSm_{0.1}O_{2-\delta}$ samples as a function of co-dopant concentration.

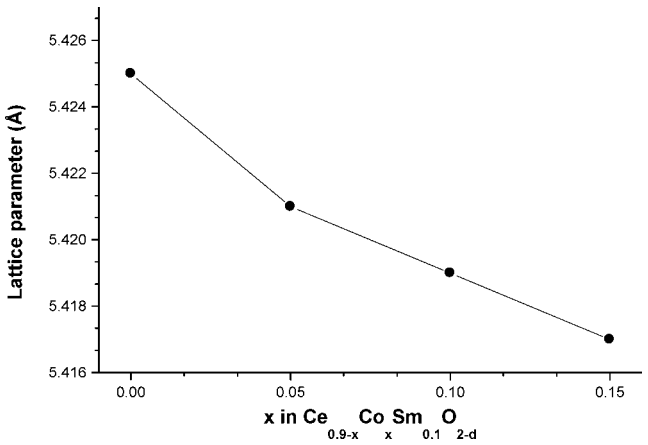

Fig. 3: Lattice parameter (Å) of $Ce_{0.9-x}Co_xSm_{0.1}O_{2-\delta}$ samples as function of co-dopant concentration.

Table 1: Lattice parameter (*a*), average crystallite size (*D*), specific surface area (S_{BET}) and average particle sizes (D_{BET}) of $Ce_{0.9-x}Co_xSm_{0.1}O_{2-\delta}$ electrolytes

Samples	Lattice parameter, *a* (Å)	Average Crystallite size, *D* (nm)	S_{BET} (m^2g^{-1})	D_{BET} (nm)
$Ce_{0.9}Sm_{0.1}O_{2-\delta}$	5.425	32.34	28.53	29.7
$Ce_{0.85}Co_{0.05}Sm_{0.1}O_{2-\delta}$	5.421	27.67	34.11	27.1
$Ce_{0.8}Co_{0.1}Sm_{0.1}O_{2-\delta}$	5.419	18.09	55.80	13.5
$Ce_{0.75}Co_{0.15}Sm_{0.1}O_{2-\delta}$	5.417	21.00	49.32	16.2

The specific surface area values are presented in Table 1. The specific area was converted to particle size (D_{BET}) in accordance with Eq. (2). From the XRD results as well as the BET measurements, it is clear that with an increasing concentration of cobalt, particle and crystallite sizes decrease, while the specific surface area increases. The possible reason behind this could be the reduction in the rate of crystal growth in ceria particles caused by the incorporation of cobalt ions into the cubic lattice of $Ce_{0.9-x}Sm_{0.1}Co_xO_{2-\delta}$.

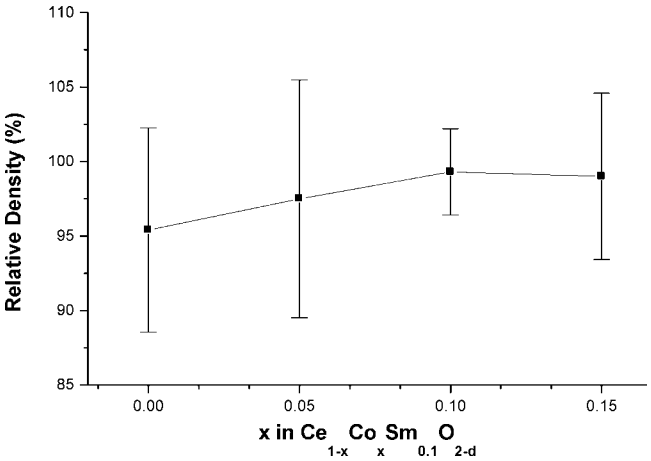

Fig. 4: Relative density of $Ce_{0.9-x}Co_xSm_{0.1}O_{2-\delta}$ at 1500 °C as a function of Co concentration (x).

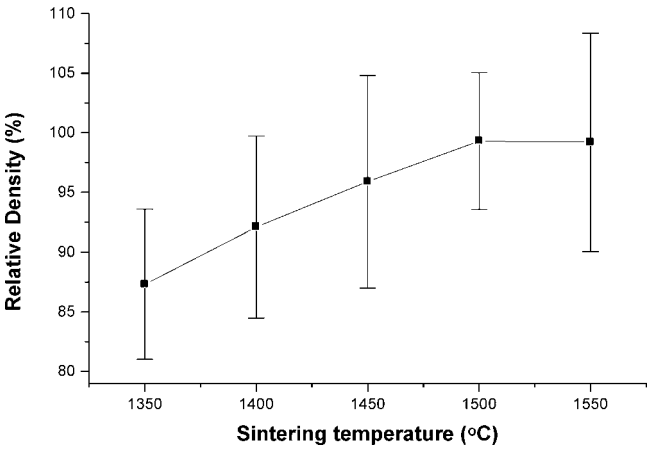

Fig. 5: Relative density of $Ce_{0.8}Co_{0.1}Sm_{0.1}O_{2-\delta}$ at different sintering temperatures.

$$D_{BET} = 6 \times 10^3 / d_{th} S_{BET} \quad (2)$$

where, d_{th} is the theoretical density of the sample (g/cm^3) and D_{BET} is the average particle size (nm).

The pellets of all the powders were sintered between the temperatures 1350 °C and 1550 °C. The effect of the cobalt concentration on the sinterability of the powders sintered at 1500 °C for 7 h is shown in fig. 4. The relative density (Table 2) of the samples sintered at 1500 °C increased with increasing cobalt concentration. The effect of the sintering temperature on the relative density of $Ce_{0.8}Co_{0.1}Sm_{0.1}O_{2-\delta}$ is shown in fig. 5. As shown in fig. 5, the densification of $Ce_{0.8}Co_{0.1}Sm_{0.1}O_{2-\delta}$ electrolytes increases with the sintering temperature from 1350 °C to 1500 °C; above 1500 °C, the densification decreases.

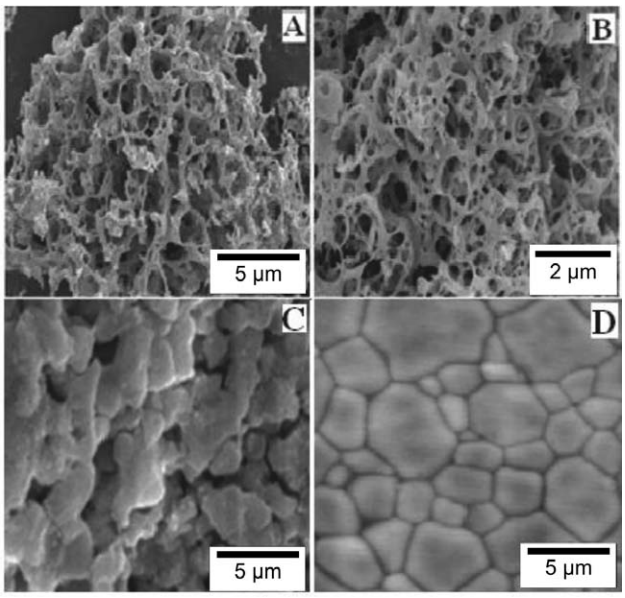

Fig. 6: SEM micrographs of the surface of $Ce_{0.8}Co_{0.1}Sm_{0.1}O_{2-\delta}$ powder (A and B), $Ce_{0.8}Co_{0.1}Sm_{0.1}O_{2-\delta}$ sintered at 1350 °C (C) and 1500 °C (D).

Fig. 6 shows SEM micrographs of $Ce_{0.8}Co_{0.1}Sm_{0.1}O_{2-\delta}$ powders and pellets sintered at 1350 °C and 1500 °C. Figs. 6A and B show the morphology of the sample at different magnification scales. It can be seen that the co-doped ceria powder calcined at 650 °C exhibits foam-like morphology. The sample sintered at 1350 °C shows relatively high porosity as compared with the sample sintered at 1500 °C. No pores are observed on the sample surface, which is consistent with the measured density of the sintered pellet.

The temperature-dependent conductivity of $Ce_{0.9-x}Co_x Sm_{0.1}O_{2-\delta}$ electrolytes sintered at 1500 °C was studied by plotting a logarithmic relationship between log(σT) and 1000/T. Pure ceria is a mixed ionic and electronic conductive material. However, the electronic conductivity of ceria can be significantly reduced with substitution of metal ions. The electrical conductivity of doped ceria is influenced by several factors, such as the dopant ion, the concentration of dopant ion, the oxygen vacancy concentration and enthalpy associated with defects. In this paper the conductivity of the co-doped samples was measured in air and treated as oxide ionic conductivity.

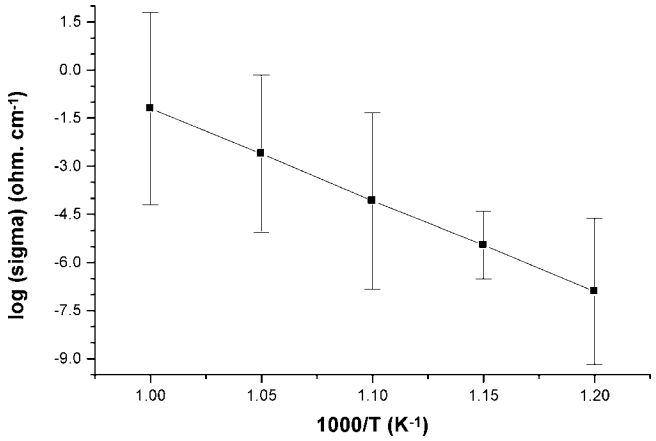

Fig. 7: Arrhenius plot for ionic conductivities of $Ce_{0.8}Co_{0.1}Sm_{0.1}O_{2-\delta}$ electrolyte sintered at 1500 °C.

It was found that the total conductivity of the sintered $Ce_{0.9-x}Co_xSm_{0.1}O_{2-\delta}$ samples followed the order: x = 0.1 >0.15>0.05>0.0. Fig. 7 shows the temperature dependence of the total conductivity for $Ce_{0.8}Co_{0.1}Sm_{0.1}O_{2-\delta}$ electrolyte. Usually, the oxygen vacancies are created owing to substitution caused by co-dopant ions, which increases the ionic conductivity. In order to introduce mobile oxygen vacancies into the ceria-based compounds, tri- or divalent dopants are added. One possible explanation for the increased conductivity with the cobalt concentration is that cobalt ions incorporated into the lattice of $Ce_{0.9}Sm_{0.1}O_{2-\delta}$ create oxygen vacancies.

The activation energy for conduction is obtained by plotting the ionic conductivity data in the Arrhenius relation for thermally activated conduction. Activation energy can be calculated in accordance with the Arrhenius equation (Eq. 3):

$$\sigma = \sigma_o/T) \exp(-E_a/k_BT) \quad (3)$$

where k_B is Boltzmann's constant, σ_o is a constant related to the density of the charge carriers i.e. oxide vacancies, E_a is activation energy for ionic migration. The conductivity of ceria-based compounds in air is mainly due to oxide ionic conductivity while the contribution of electronic conductivity is negligible[15]. On formation of mobile oxygen vacancies, the ionic conductivity dominates the electronic conductivity. It was observed that the oxide ion mobility increases with increasing temperature, which in turn increases the conductivity at high temperatures. The activation energy for conduction is obtained by plotting the ionic conductivity data in Eq. 2. Fig. 8 shows the variation of activation energy with the cobalt concentration in $Ce_{0.9-x}Co_xSm_{0.1}O_{2-\delta}$ solid electrolytes. It can be seen that, as the concentration of cobalt increases from x = 0.00-0.1, the activation energy tends to decrease from 0.89 to 0.81 eV. The minimum value of activation energy (0.81 eV) was observed for the composition $Ce_{0.8}Co_{0.1}Sm_{0.1}O_{2-\delta}$ (Table 2). Such a decrease in activation energy is attributed to the presence of attractive interactions between dopant cations and oxygen vacancies. For the cobalt concentration x = 0.15 in $Ce_{0.9-x}Co_xSm_{0.1}O_{2-\delta}$ electrolytes, the activation energy increases, causing the reduced oxygen ionic conductivity. The ionic conductivity depends mainly on the mobile oxygen concentration. At higher dopant concentration, the reduced ionic conductivity is the result of the formation of local defect structure[11] and lower mobile oxygen vacancy concentration.

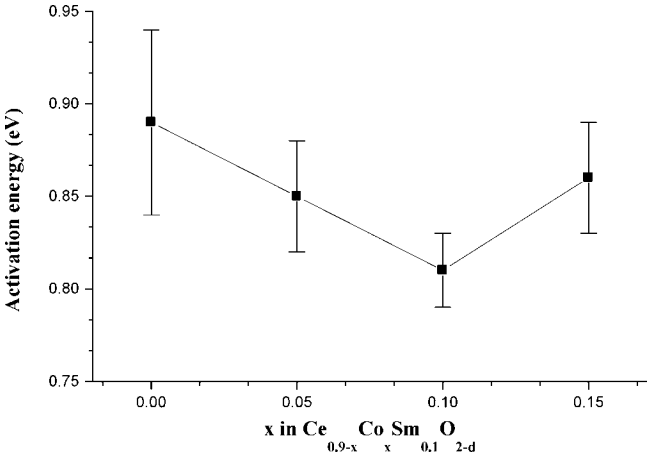

Fig. 8: Activation energy (eV) of $Ce_{0.9-x}Co_xSm_{0.1}O_{2-\delta}$ electrolytes (sintered at 1500 °C) as a function of the cobalt concentration.

Table 2: Activation energies (Ea) and relative densities of $Ce_{0.9-x}Co_xSm_{0.1}O_{2-\delta}$ electrolytes.

Samples	Relative density (%) (sintered at 1500 °C)	Activation Energy (Ea)
$Ce_{0.9}Sm_{0.1}O_{2-\delta}$	95.4±6.8	0.89±0.05
$Ce_{0.85}Co_{0.05}Sm_{0.1}O_{2-\delta}$	97.5±7.9	0.85±0.03
$Ce_{0.8}Co_{0.1}Sm_{0.1}O_{2-\delta}$	99.3±2.9	0.81±0.02
$Ce_{0.75}Co_{0.15}Sm_{0.1}O_{2-\delta}$	99±5.5	0.86±0.03

IV. Conclusions

To summarize, $Ce_{0.9-x}Co_xSm_{0.1}O_{2-\delta}$ nanoparticles were successfully prepared with the EDTA-glycol method. The crystal structure of all the samples calcined at 650 °C was fluorite. The synthesized nanocrystals have the diameters in the range of 18-32 nm. It was found that the cobalt concentration in $Ce_{0.9-x}Co_xSm_{0.1}O_{2-\delta}$ samples affected the density. The relative density of $Ce_{0.8}Co_{0.1}Sm_{0.1}O_{2-\delta}$ sample was found to be the highest. The formation of the small particle size of the $Ce_{0.9-x}Co_xSm_{0.1}O_{2-\delta}$ samples is the reason for the reduced sintering temperature at 1500 °C. The effects of cobalt co-doping are clearly reflected by the changes in the density and activation energy of $Ce_{0.9}Sm_{0.1}O_{2-\delta}$ solid electrolyte.

Acknowledgement

The author is grateful to the Department of Metallurgy and Material Science Engineering, VNIT Nagpur for permitting the use of the XRD and SEM measurements.

References

1 Minh, N.Q., Ceramic Fuel Cells, *J.Am.Ceram.Soc.*, **76**, 563-588, (1993).

2 Zha, S., Xia, C., Meng, G., Effect of Gd (Sm) doping on properties of ceria electrolyte for solid oxide fuel cells, *J. Power sources* **115**, 44-48, (2003).

3 Wei, X., Pan, W., Cheng, L., Li, B., Atomistic calculation of association energy in doped ceria, Solid State Ionics, **180**, 13-17, (2009).

4 Yahiro, H., Eguchi, Y., Eguchi, K., Arai H., Oxygen ion conductivity of the ceria-samarium oxide system with fluorite structure, *J. Appl. Electro-Chem.*, **18**, 527-531, (1988).

5 Kochi, E., Ceramic materials containing rare earth oxides for solid oxide fuel cell, *J. Alloys and Compounds*, **250**, 486-491, (1997).

6 Bryan, G., Glass, R.S., ac impedance studies of rare earth oxide doped ceria, Solid State Ionics, **76**, 155-162, (1995).

7 Wang, F.Y., Chen, S., Cheng, S., Gd^{3+} and Sm^{3+} co-doped ceria electrolytes for intermediate temperature solid oxide fuel cells, *J. Electrochem Commun.*, **6**, 743-746, (2004).

8 Ralph, J.M., Przydatek, J., Kilner, J.A., Seguelong, T., Novel doping system in ceria, Ber. Bunsenges. Phys. Chem., **101**, 1403-1407, (1997).

9 Yoshida, H., Deguchi, H., Miura, K., Horiuchi, M., Investigation of the relationship between the ionic conductivity and the local structures of singly and doubly doped ceria compounds using EXAFS measurement, Solid State Ionics, **140**, 191-199, (2001).

10 Mori, T., Drennan, J., Lee, J.H., Li, J.G., Ikegami, T., Oxide ionic conductivity and microstructures of Sm- or La-doped CeO_2-based systems, Solid State Ionics, 154-155, 461-466, (2002).

11 Yoshida, H., Inagaki, T., Miura, K., Inaba, M., Ogumi, Z., Density functional theory calculation on the effect of local structure of doped ceria on ionic conductivity, Solid State Ionics, **160**, 109-116, (2003).

12 Kleinlogel, C., Gauckler, L.J., Sintering of Nanocrystalline CeO_2 Ceramics, Adv. Mater., **13** (14), 1081-1085, (2001).

13 Azimova, M.A., McIntosch, S., Transport properties and stability of cobalt doped proton conducting oxides, Solid State Ionics, **180**, 160-167, (2009).

14 Pawar, M.J., Gas sensing behavior of $LaMnO_3$ ceramic, *J. Opt. Adv. Mate.*, **9** (12) 3785-3789, (2007).

15 Inaba, H., Tagawa, H., Ceria based solid electrolytes, Solid State Ionics, **83**, 1-16, (1996).